FOI-R--0275--SE
December 2001
ISSN 1650-1942
Scientific Report

Cesar Lopes, Bertil Eliasson, Christina Nilsson,
Patrick Norman, Hans Ågren and Anders Eriksson

Synthesis, Theoretical Modeling and Characterization of Optical Limiting Materials

Sensor Technology
SE-581 11 Linköping

SWEDISH DEFENCE RESEARCH AGENCY

Sensor Technology
P.O. Box 1165
SE-581 11 Linköping

FOI-R--0275--SE

December 2001

ISSN 1650-1942

Scientific Report

Cesar Lopes[1], Bertil Eliasson[2], Christina Nilsson[1],
Patrick Norman[3], Hans Ågren[4] and Anders Eriksson[1]

Synthesis, Theoretical Modeling and Characterization of Optical Limiting Materials

1) FOI, Swedish Defence Research Agency
Sensor Technology
Department of Functional Materials

2) Department of Chemistry, Organic Chemistry
Umeå University, Umeå

3) Department of Physics and Measurement Technology
Linköping University, Linköping

4) Theoretical Chemistry
Royal Institute of Technology, Stockholm

Issuing organization	Report number, ISRN	Report type
FOI – Swedish Defence Research Agency Sensor Technology P.O. Box 1165 SE-581 11 Linköping Sweden	FOI-R--0275--SE	Scientific report
	Research area code 6. Electronic Warfare	
	Month year December 2001	**Project no.** E3021, E3826
	Customers code 5. Contracted Research	
	Sub area code 61. Electronic Warfare, Electromagnetic Weapons	

Author/s (editor/s)	Project manager
Cesar Lopes, Bertil Eliasson, Christina Nilsson, Patrick Norman, Hans Ågren and Anders Eriksson	Sören Svensson
	Approved by
	Sponsoring agency Swedish Armed Forces
	Scientifically and technically responsible Cesar Lopes

Report title

Synthesis, Theoretical Modeling and Characterization of Optical Limiting Materals

Abstract (not more than 200 words)

The "Photonics in defense applications" program is a collaboration between FOI, Universities and industries in Sweden. One of the projects within this program is "Technical demonstration of electro-optical counter counter-measures." The goal for this 3-year project is to incorporate protective devices within a model sight with the aim to protect the human eye against laser damage. This report gives a short introduction to the project and summarizes the results obtained on passive optical limiters during the first project year. The optical limiting performance of the compounds was investigated with the dyes in solution. The solutions were prepared with a photopic transmission of approximately 70%. Eleven new compounds were investigated. The investigations were performed with a frequency doubled Nd:YAG delivering 5 ns pulses at 532 nm. A tunable laser with an optical parametric oscillator (OPO) was also used to perform measurements at various wavelengths. A f/5 arrangement was used in the experiments. A mixture of alkynylplatinum(II), with a photopic transmission of 68%, gave the best result; clamping values <1μJ were observed for a major part of the visible wavelengths.

Keywords

Optical limiting, synthesis, theoretical modeling

Further bibliographic information	Language English
ISSN 1650-1942	**Pages** p. 38
	Price acc. to pricelist

Utgivare	Rapportnummer, ISRN	Klassificering
Totalförsvarets Forskningsinstitut - FOI	FOI-R--0275--SE	Vetenskaplig rapport
Sensorteknik	**Forskningsområde**	
Box 1165	6. Telekrig	
581 11 Linköping	**Månad, år**	**Projektnummer**
	December 2001	E3021, E3826
	Verksamhetsgren	
	5. Uppdragsfinansierad verksamhet	
	Delområde	
	61. Telekrigföring med EM-vapen och skydd	

Författare/redaktör	Projektledare
Cesar Lopes, Bertil Eliasson, Christina Nilsson, Patrick Norman, Hans Ågren och Anders Eriksson	Sören Svensson
	Godkänd av
	Uppdragsgivare/kundbeteckning FM
	Tekniskt och/eller vetenskapligt ansvarig Cesar Lopes

Rapportens titel (i översättning)

Syntes, Modelering och Karakterisering av Optiska Begränsare

Sammanfattning (högst 200 ord)

Inom FMVs fotonikprogram samarbetar FOI, universitet och högskolor samt försvarsindustrin med att ta fram demonstratorer. Ett av projekten inom fotonikprogrammet är "Teknisk demonstration av skydd mot laser." Målet med projektet är att inom 3 år ta fram och bygga in skyddskomponenter, för skydd av ögon, i ett sikte. Rapporten ger en kort introduktion till projektet och summerar resultaten från projektstarten december 2000 fram till idag, med avseende på skydd mot skada (optisk begränsning). Experimenten genomfördes med föreningarna i lösning. Den fotopiska transmissionen för de olika lösningarna var ca. 70%. 11 nya föreningar framställdes och undersöktes. Experimenten med avseende på optisk begränsning gjordes med en Nd:YAG laser med pulslängden 5 ns, eller en avstämbar laser med OPO, i en f/5 testuppställning.
För skydd av ögon krävs material som klarar av att begränsa laserljuset till ≤ 1 μJ. En blandning bestående av alkynylplatina(II) föreningar, med en fotopisk transmission av 68%, begränsade den transmitterade energin till < 1 μJ för en stor del av det synliga området.

Nyckelord

Optisk begränsning, framställning, modelering

Övriga bibliografiska uppgifter	Språk Engelska
ISSN 1650-1942	**Antal sidor:** s. 38
Distribution enligt missiv	**Pris: Enligt prislista**

Content

2. Introduction and background 5
1.1. Electro-optical counter countermeasures; passive optical limiters 5
1.2. Laser induced damage to sensors 7
1.3. Incorporation of optical limiters within a model sight 8

2. Experimental 10
2.1. The optical limiting test-bed 10
2.2. UV-vis characterization 11
2.3. Synthesis and description of investigated compounds 12
2.3.1. Alkynylplatinum(II) complexes and alkyne precursors for platinum(II) complexes 12
2.3.2. Di- and trialkynylthiophenes 13
2.3.3. Thiacalix[4]arenes and Porphyrins 15

3. Results 16
3.1. Linear and non-linear absorption 16
3.2. Theoretical modeling 20
3.2.1. Methodological development 20
3.2.1.1. Role of coherent one-step versus incoherent two-step absorption for optical limiting 20
3.2.1.2. Generalized few-state models for two-photon absorption 21
3.2.1.3. Development of propagator techniques for calculating the incoherent transition cross-sections 22
3.2.2. Applications 22
3.2.2.1. Use of effective core potentials for NLO properties 22
3.2.2.2. Effects of relativity on linear and nonlinear polarazabilities 22
3.2.2.3. Effects of π-centers and symmetry on one step two-photon absorption cross sections of organic chromophores 23
3.2.2.4. One and two-photon spectra of systematic donor/acceptor substituted alkynylplatinum(II) compounds 24
3.2.2.5. Density functional theory for nonlinear optical processes in porphyrin based donor/acceptor systems 25
3.2.2.6. Photo-oxidation products of two-photon absorbers (AF30) 25
3.2.2.7. Figures of merit for some charge transfer systems 26

4. Discussion 29

5. Measurement uncertainties 30

6. References 30
Appendix I. Synthesis 31

1. Introduction and Background

The "Photonics in defence applications" program, initiated by FMV, is a collaboration between FOI, national and international Universities, and industries in Sweden.
One of the projects within this program is "Technical demonstration of electro-optical counter countermeasures" (EOCCM). This report gives a short introduction to the EOCCM-project and summarizes the results obtained on passive optical limiters during the first project year.

1.1 Electro-optical counter countermeasures; Passive optical limiters

During the last decade there has been an increasing interest in nonlinear optical (NLO) power limiting materials. One driving force behind the increased attention is the military application of these materials. Optical limiting means that a material, through the nonlinear absorption mechanism, show an increased absorption with increasing laser irradiance or fluence. And, as the incident optical power increases, the transmitted energy is clamped to below a certain value; the transmitted energy is constant (Figure 1.1.1).

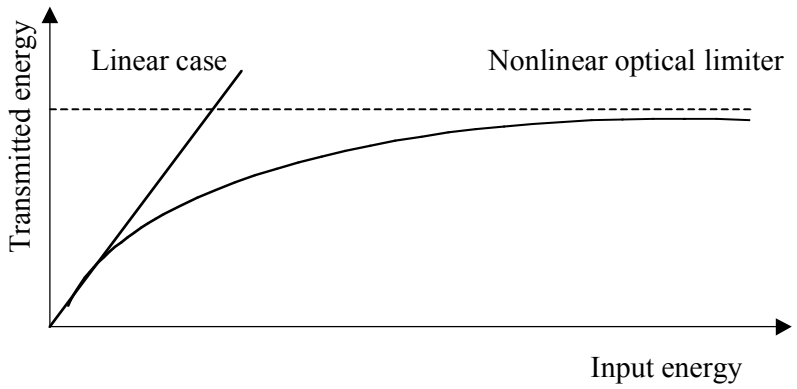

Figure 1.1.1*. Schematic figure of the response of a nonlinear optical limiter.*

This means that optical limiters can provide eye and electro-optical sensor protection from lasers, if the transmitted energy is clamped below the damage threshold of the sensor.
In order to access the nonlinear limiting effect, the materials need to experience a high intensity. A sight, for instance, offers the optical design, *i.e*. a focal plane, needed to generate the required intensity. This is also the goal for this project "Technical Demonstration of Electro-Optical Counter Countermeasures"; incorporation of protective devices within a model sight, with the aim to protect the human eye.

Laser weapons against eyes and electro-optical sensors can be divided into two distinct categories:

- Laser weapons designed to dazzle or jam, and,
- Laser weapons designed to permanently damage the human eye or electro-optical sensors.

Cw (continuous wave) lasers are most likely used to dazzle or jam, while pulsed laser weapons are more likely used to damage. In order to achieve protection against dazzle and damage, active protection devices and passive optical limiters are needed. Passive means that the optical energy itself is responsible for activation of the material. Active protection devices, *e.g*. shutters, on the other hand, require a trigger signal for activation, and, therefore are not quick enough to block the first laser pulses. In this report the focus is on sensor protection against damage, *i.e.* passive optical limiters; in particular optical limiters for application at visible wavelengths (~400 - ~700 nm).

During the last decade promising materials for optical limiting have been presented [1]. Materials such as alkynylplatinum(II) [2], metallophthalocyanines [3], and carbon black suspensions [4] have been thoroughly investigated. Still, there is a need of better optical limiting materials to satisfy the military requirements.
Based on earlier investigations promising materials were chosen for use as optical limiters or matrix materials. These are:

- Coordination compounds; alkynylplatinum(II), porphyrins, and, metallo - thiacalixarenes.
- Organic compounds; thiophenes, dendrimers and hyperbranched fluorinated polymers.

The project goals concerning passive optical limiters are:

- The nonlinear optical limiter should limit the energy to ≤1 μJ
- The material (or a mixture of materials) should act as a broad-band optical limiter in order to cover the operating waveband of the sensor
- The material (or a mixture of materials) should possess high linear transmission

The devices needed to protect eyes behind an optical sight will cause transmission loss. High linear transmission means that the complete protection device (the passive optical limiter and the active protection device), working together, should give a linear transmission of at least 50%.
Our intention is also that the protective devices shall work against realistic laser threats, *e.g*. frequency doubled Nd:YAG (ns pulses) and dye lasers (μs pulses).
The final demonstration, with the built-in protective devices within the model sight, will be performed indoors at the end of year 2003.

1.2. Laser induced damage to sensors

One of the most difficult "sensors" to protect is the human eye. Figure 1.2.1 depicts how light is focused on the retina through the magnifying optics in the eye.

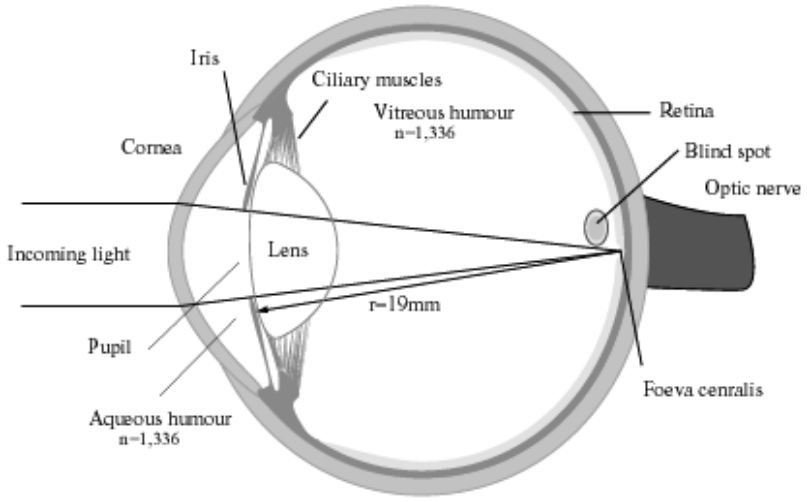

Figure 1.2.1. *A light-beam focused on the retina of the eye.*

The eye is a complex and precise optical system of the size ~25 mm in diameter. When light enters the eye, it first passes through the cornea, a living tissue exposed directly to environmental elements. The cornea is protected from drying out by the tear film. The cornea focuses the major part of the light on the rear of the eye. Once the light has passed through the cornea, it enters the aqueous humour. The next part is the pupil which can be adjusted in size by the iris, the colored part of the eye. The size of the pupil can be adjusted from approximately two to seven millimetres in response to the average illumination of the light. The colorless lens, directly behind the iris, does not absorb within the visible light. After the light has passed the lens, it goes though the vitreous humour, a colorless gel. The vitreous body is attached to the ciliary body and to the retina at several points. When the light has passed the vitreous body it finally hits the retina. A single cell layer called the retinal pigment epithelium (RPE) covers the outer surface of the retina. Two types of photoreceptor cells, rods and cones, are placed just inside this layer.
The amount of light reaching the retina can be adjusted by contracting and expanding the pupil of the iris. The cillary muscles, on the other hand, can change the shape of the lens and, thus, focus the incoming light to form a sharp image on the retina.

A laser beam, with wavelengths between 400 and 1400 nm, entering the human eye can experience an irradiance gain of ~100 000 times at the retina [5]. The beam is focused to a diameter of ~10 µm This gives a very high fluence at the focusing spot on the retina, which, through thermal or photochemical processes, may lead to damage to retinal cells.

The MPE (maximum permissible exposure) recommended by the European Laser Safety Standard is 0.5 μJ/cm^2 (~0.2 μJ entering the eye) at the cornea . The ED_{50} value, which corresponds to a 50% probability of injury to occur, is ~2.8 μJ at the cornea. For single laser pulses (1 ns - 20 μs) in the wavelength range 400 - 700 nm, we adopt 1 μJ, at the cornea, as an approximation of the energy that the eye can sustain without being damaged.
The damage thresholds for solid state sensor detectors are usually of the same order of magnitude as for the human retina.

1.3. Incorporation of optical limiters within a model sight

Optical equipment is used by the military personal for many purposes, *e.g.* observation, navigation, fire control, and reconnaissance. The laser, on the other hand, is a powerful countermeasure weapon against optical equipment, particularly the detectors. For instance, as mentioned above, in-band laser radiation is a major threat to eyes, and especially, eyes behind magnifying optics. The solution to this threat is to incorporate optical limiters within the optical equipment. Useful optical limiters are, nevertheless, colored, which means transmission loss, due to linear absorption.
A combination of materials, a mixture, can give some relieve to this problem since a "cocktail" of dyes with complimentary colors can appear color neutral. Mixtures are also useful for achieving broad-band optical limiting.

In this project a model sight, designed with brackets for accommodation of optional components, *e.g.* protective devices (passive and active devices) will be used. A sketch of the model sight is depicted in figure 1.3.1.

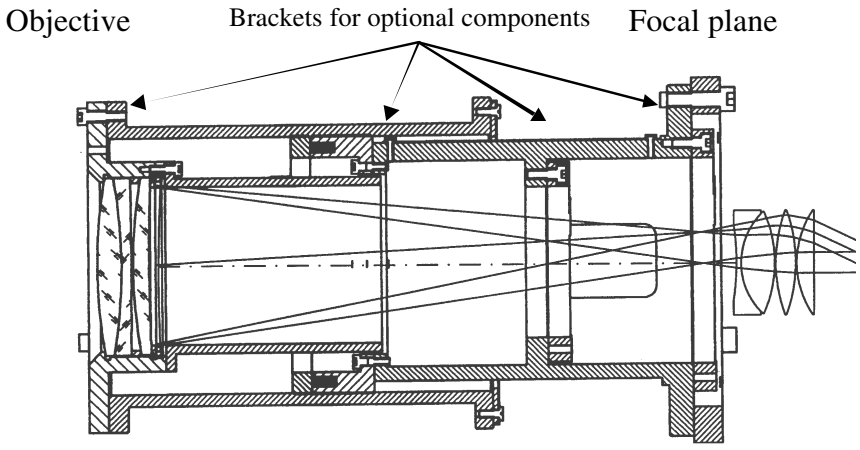

Figure 1.3.1. *A sketch of the model sight*

The focal plane is utilized for accommodation of the passive optical limiter in order to achieve the high intensity and small spot size required. The spot size and the focus position inside the cell containing the passive material are important for the performance of the optical limiter. A small spot size gives a high intensity, which is necessary for achieving the required clamping. As can be seen in figure 1.3.2 the position of the focus inside the cell is likewise important for the clamping level. The focus should remain at the best position within the cell and maintain a good enough quality to ensure low clamping levels.

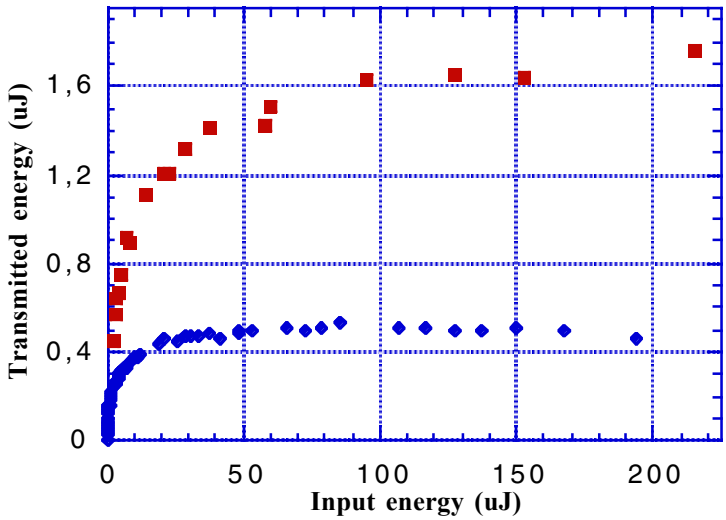

Figure 1.3.2. *The transmitted energy is dependent on the position of the focus in the cell. The optical limiting with the focus at the best position, (blue), and the focus set closer to the rear of the cell, (red). The measurements were performed in a f/5 arrangement with an Nd:YAG laser giving 5 ns pulses at 532 nm*

The focusing of the laser beam into a cell containing the optical limiting material can cause decomposition of the material. For liquid-phase limiters, self-healing is a possibility because of diffusion. Laser induced damage of compounds in a solution can create solid particles which can further reduce the transmitted energy, *i.e.* giving sacrificial protection. Solid materials lack the self-healing capacity.
The cell containing the liquid is also at risk of being damaged. Deposition of particles on the front window of a cell may cause damage to the cell.
Since the demonstration will be indoors, we will not discuss military requirements, such as sensitivity to vibration or temperature.

2. Experimental

2.1. The optical limiting test-bed

Before the optical limiting device can be incorporated within the model sight, the materials have to be characterized and tested. For this purpose a test-bed consisting of the same optical arrangement as the model sight (f/3.7) as well as a test-bed with an f/5 [6, 7] configuration is used (Figure 2.1.1).

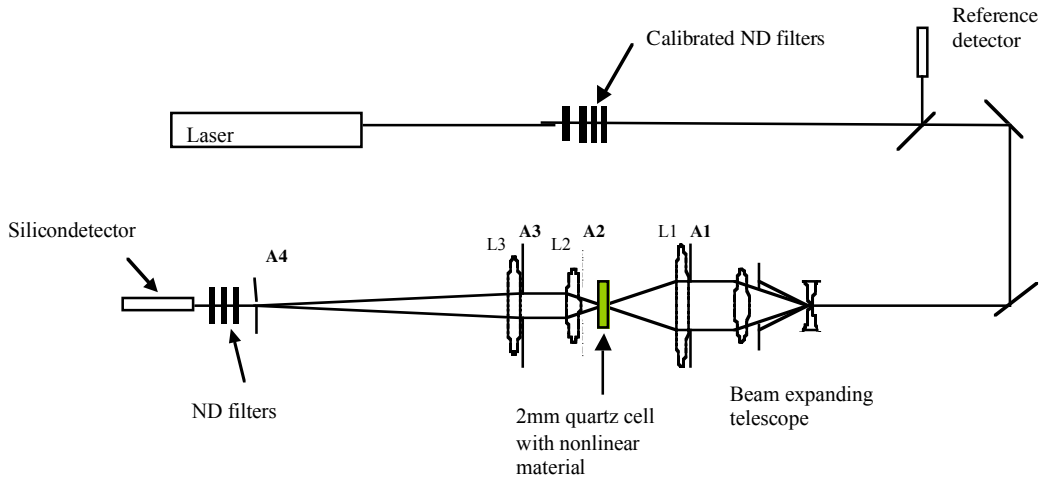

Figure 2.1.1. *Test bed arrangement for assessment of the nonlinear protective properties of materials.*

One of the reasons for using the f/5 configuration is that it is an internationally accepted standard test-bed.
Initially the f/3.7 arrangement was also used in the characterizations. Figure 2.1.2 shows a beam expander and the corresponding model sight lenses in the set-up. A 2 mm quartz cell, situated at the focal plane between the objective and ocular, is also seen in this picture.

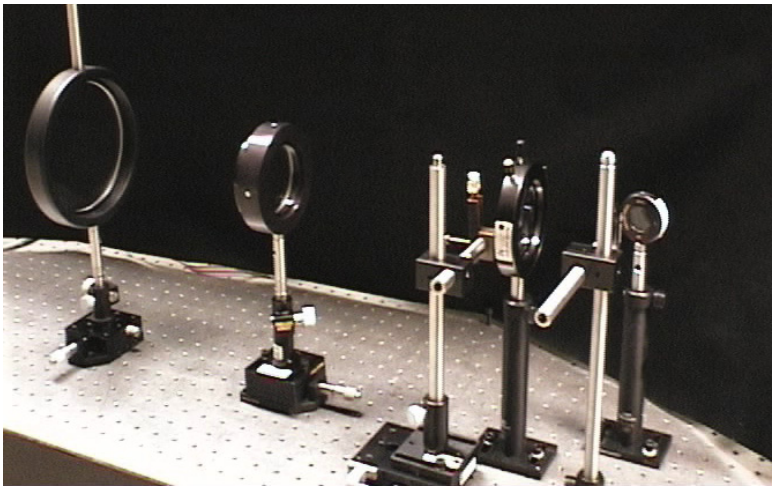

Figure 2.1.2. *The f/3.7 test-bed arrangement.*

With a laser beam propagated over a long distance an even illumination of the sight can be expected (ignoring turbulence effects). A uniform illumination of the objective was achieved with a beam expanding telescope in front of the test-bed in order to resemble a laser beam from a distant source. It was however found that when the tunable laser was used the beam profile was very poor and a perfectly even illumination was not possible to obtain without loosing too much energy. Only a few experiments were conducted with the f/3.7 system. This system needs to be optimized before it can be used to in the experiments. The measurements were therefore performed with the f/5 arrangement. The compounds were solubilized in an appropriate solvent and the solutions were filtered prior to the optical limiting measurements. The cell with the nonlinear material under investigation was positioned with the focus centered in the cell. A frequency doubled Nd:YAG laser delivering 5 ns pulses at 532 nm with a repetition rate of 10 Hz was used in the investigations. A tunable laser with an optical parametric oscillator (OPO) was also used to perform measurements at various wavelengths between 450 nm and 650 nm.

2.2. UV-vis characterization

The transmission spectra were recorded with a CARY 5G UV-VIS-NIR spectro-photometer. The spectra show the transmission related to the wavelength for both cell and solution.
Since the priority is protection of the eye against laser induced damage, photopic transmission (PT) will be used throughout this work. The photopic transmission is the product of the spectral luminous efficiency of the eye and percent transmission of a material.

2.3. Synthesis and description of investigated compounds

Detailed description of the synthesis procedures can be found in Appendix I.

2.3.1. Alkynylplatinum(II) complexes and alkyne precursors for platinum(II) complexes

Alkynylplatinum(II) compounds with the concise formula $Pt(C\equiv C\text{-}Ar\text{-}R)_2L_2$ (Figure 2.3.1.1, and 2.3.1.2), and $Pt(C\equiv C\text{-}Ar)ClL_2$ (Figure 2.3.1.2) have been prepared.

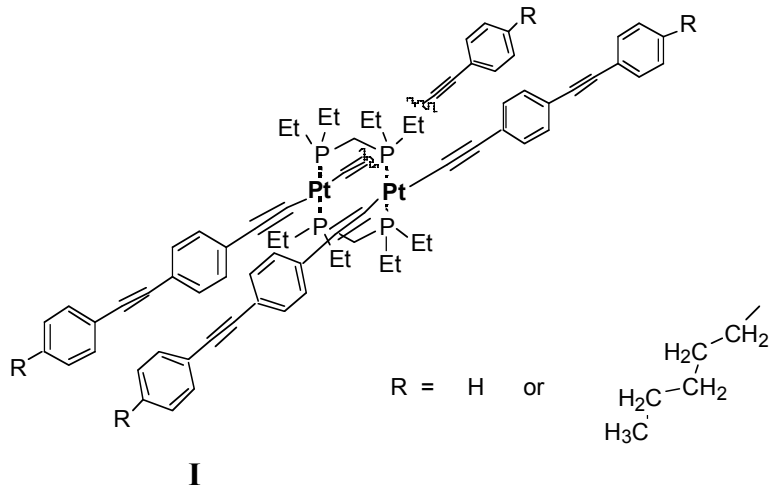

I

Figure 2.3.1.1*. Dimer of alkynylplatinum(II) , compound* ***I***

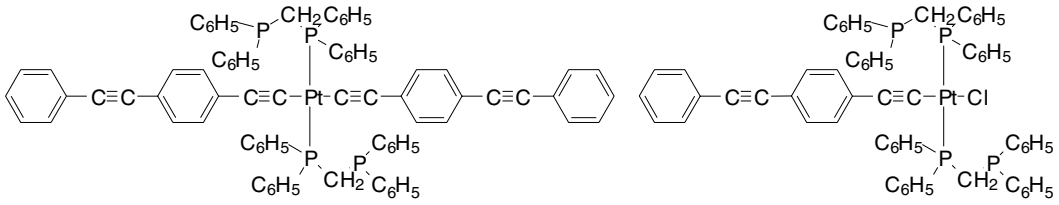

II **III**

Figure 2.3.1.2. *Monomers of alkynylplatinum(II)*

The atomic arrangement in this class of compounds is briefly described as follows: In general, R (in the formulas) denotes hydrogen or an alkyl chain, which can be altered by synthesis to improve solubility in commonly used solvents. In case of hydrogen or an alkyl group, R is thought to have little effect on the electronic properties of the compound. However, if strong electron donors or acceptors, such as NH_2 or NO_2 groups, are placed in the R positions, significantly altered molecular properties are expected. Theoretical modeling of other compounds, as described in section 3.2,

reinforces this assumption. Ar denotes various unsaturated units, which are important for the optical limiting capability of the molecule. The Ar-group has an all-carbon π-electron system in the synthesized compounds, but will have other atoms, such as sulfur, in compounds that are underway. The Ar group is connected to the Pt center via an ethynyl group. However, the ethynyl is also important for the electronic communication within the Ar unit, and Ar can also contain one or more ethynyl groups. The L group is preferably a phosphine ligand, which stabilizes the complex. In addition, the nature of L can influence the solubility and the electronic properties of the compounds. Nitriles and other L groups are also considered in this project.
Two of the prepared compounds (with R = H or *n*-C_5H_{11}) are believed to have a dimeric structure as indicated in figure 2.3.1.1. More information on the monomer-dimer equilibrium is expected from ^{31}P and ^{195}Pt NMR studies in the near future.
The Pt compounds have been characterized by ^{1}H and ^{13}C NMR and IR spectroscopy. Synthetic details are given in the appendix.

Two new alkynes have recently been prepared in order to obtain two goal platinum(II) complexes (Figure 2.3.1.3). The scheme below shows the alkynes and the goal compounds. Synthesis of the Pt complexes are in progress.
The two alkynes have been characterized by ^{1}H / ^{13}C NMR and IR spectroscopy. Synthetic details are given in the appendix.

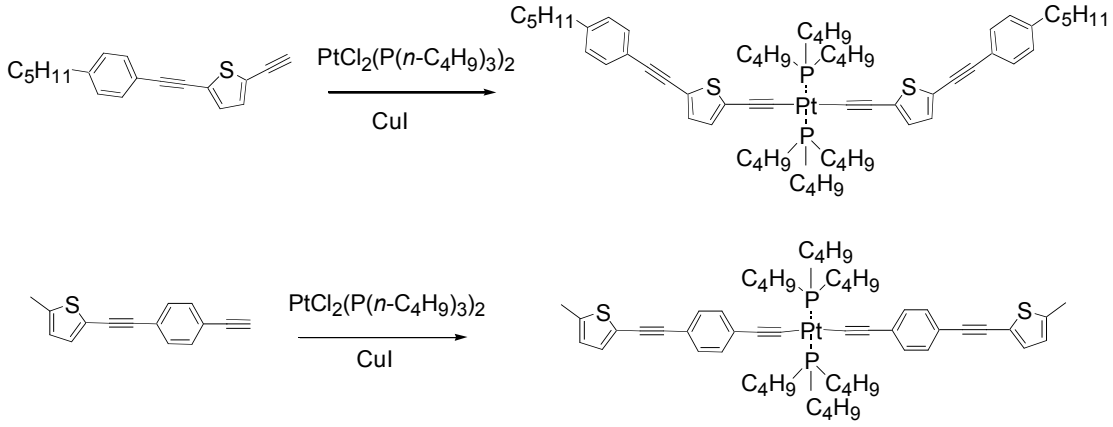

Figure 2.3.1.3. *Pt (II) complexes with thiophene based alkynyl ligands*

2.3.2. Di- and tri-alkynylthiophenes

The synthesis of three dialkynylsubstituted thiophenes (Figure 2.3.2.1) has been accomplished according to the project plan. The synthetic procedure was outlined in the earlier part of the Photonics in Defence Applications program. However, the solubility of the early compounds was generally low. The new thiophene molecules have C_5H_{11} and $C_{12}H_{25}$ alkyl tails introduced to improve solubility.

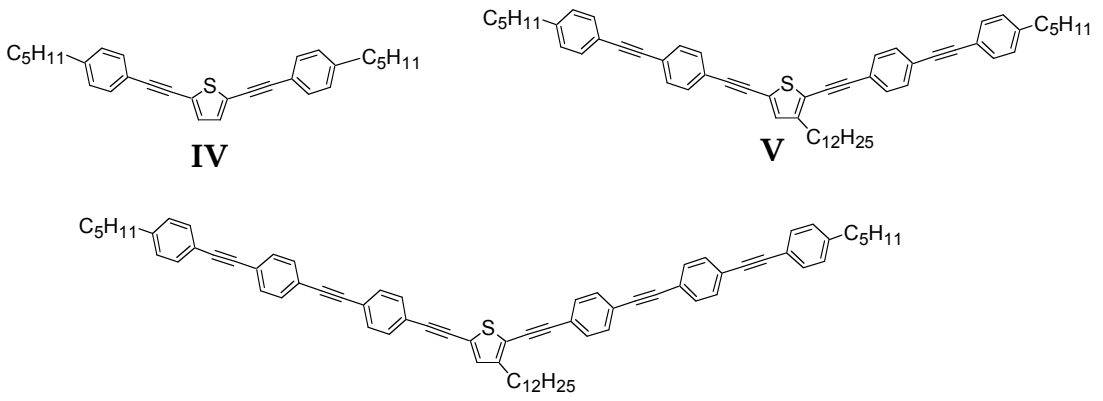

Figure 2.3.2.1. Dialkynylsubstituted thiophenes. 2,5-Di(2-(4-pentylphenyl)ethynyl)-thiophene (**IV**), 3-*n* -dodecyl-2,5-di(2-(4-(2-(4-pentylphenyl)ethynyl)phenyl)-ethynyl)thiophene (**V**) and, 3-*n* -dodecyl-2,5-di-(2-(4-(2-(4-(2-(4-pentylphenyl)-ethynyl)phenyl)ethynyl)phenyl)ethynyl)thiophene (**VI**).

The compounds have good transmission in the visible region and show good optical limiting.

A newly prepared dialkynylsubstituted thiophene having nitro groups in the thiophene ring and amino groups at the end of the alkynyl system is depicted in figure 2.3.2.2.

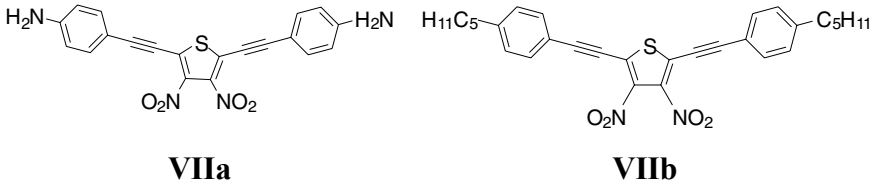

Figure 2.3.2.2*. Nitro substituted dialkynyl thiophenes*

The synthesis of a trialkynylsubstituted thiophene has also been accomplished, see figure 2.3.2.3.

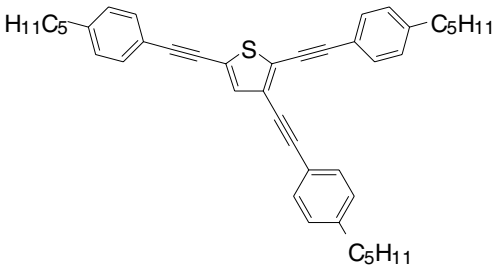

Figure 2.3.2.3. *A trialkynylsubstituted thiophene*

All thiophenes have been characterized by ^{1}H / ^{13}C NMR and IR spectroscopy. Synthetic details are given in the appendix.

2.3.3. Thiacalix[4]arenes and Porphyrins

Calixarenes, thiacalixarenes, and, porphyrins are macrocyclic compounds with extended π-delocalization.
Thiacalixarenes are very similar to calixarenes. In thiacalixarenes the original methylene bridges between the aryl units in calixarene are substituted for sulfur bridges. The syntheses of one of the thiacalixarenes is summarized in figure 2.3.3.1. The products were characterized using the usual techniques: NMR, Mass spectrometry, FT-IR, single crystal X-ray diffraction, and DSC.

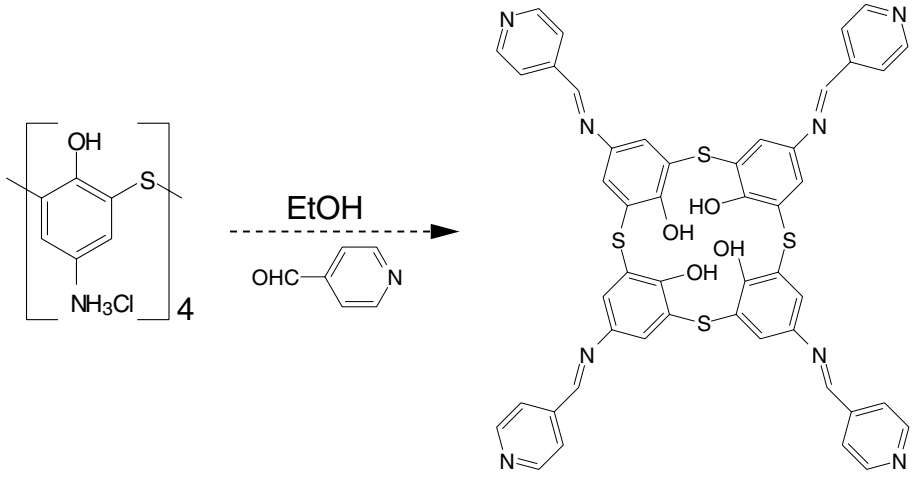

IX

Figure 2.3.3.1. *Synthesis of tetra(4-pyrydylimino)-tetrahydroxythiacalix[4]arene (**IX**)*

Thiacalix[4]arenes are in most cases soluble in common organic solvents, and are thermally very stable (up to 320°C).
The porphyrins depicted in figure 2.3.3.2 have also been used in this work.

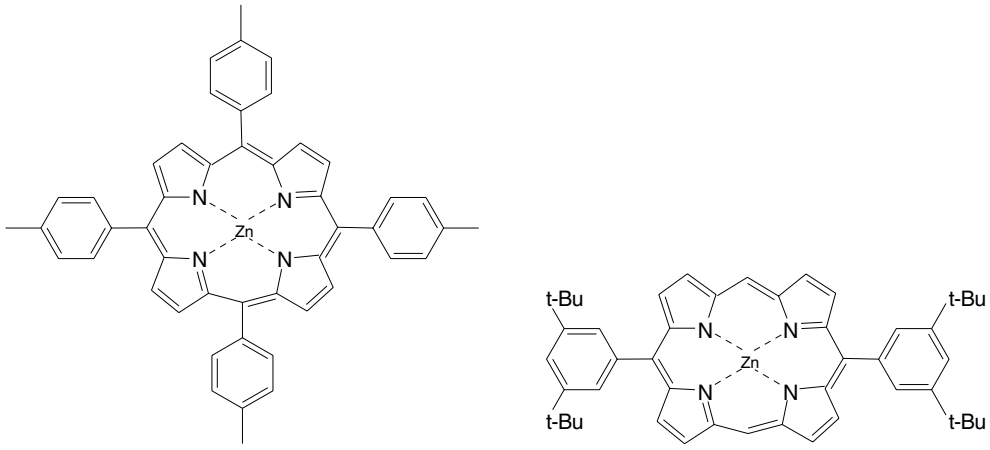

(X) **(XI)**

Figure 2.3.3.2*. Porphyrin compounds, ZnTPP (**X**) and ZnP (**XI**)*

3. Results

3.1. Linear and non-linear absorption

In this section selected results on optical limiting and linear transmission are presented. The compounds were solubilized in THF or chloroform. THF was used for compounds **I**, **II**, **IV**, **V**, and **VIII**, and chloroform for compound **VI** (see section 2.3 for description of the molecules). Compound **VIII** is an oil at room temperature. This oil was diluted with THF. Throughout this work 2 mm quartz cells were used in the investigations. The optical limiting investigations were performed in a f/5 arrangement.

The photopic transmissions were calculated for the solutions. Figure 3.1.1 shows the relative luminous efficiency of the eye [8], the UV-vis transmission of a mixture of alkynylplatinum(II) compounds (**MIX I**) dissolved in chloroform, and the resulting photopic transmission.

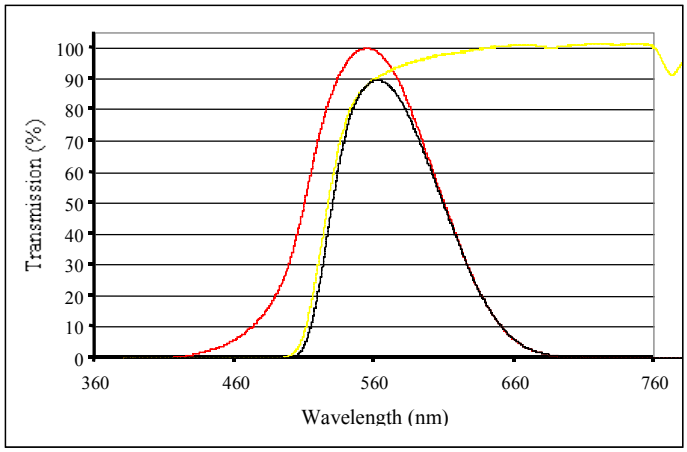

Figure 3.1.1*. The relative luminous efficiency of the eye (red), the linear transmission of a solution of alkynylplatinum(II) compounds,* ***MIX I*** *(yellow), and the photopic transmission (black).*

The linear transmission depicted in figure 3.1.1 is also representative for all the investigated solutions. In accordance with the project plan, and if it was possible, the solutions were prepared in order to give a photopic transmission of approximately 70%.
Selected results on linear transmission and clamping values are given in table 3.1.1.

Compound	% T @ 532 nm	% PT	CL (µJ) @ 450 nm	CL (µJ) @ 532 nm	CL (µJ) @ 650 nm
I	64.7	70	0.4*	5	14
II	70	73	-	7	-
IV	87.5	85	3	7.8	22
V	92	87.5	1.7	11.5	11
VI	97	89	0.1	13	14
VIIb	66.5	70	0.005*	7	14
VIII	70	72.4	1*	7	7

%T = % transmission, %PT = % photopic transmission, CL = Clamping level. * = CL @ 480 nm

***Table 3.1.1**. Experimental results on the thiophenes*

A more detailed investigation of the clamping values for the thiophenes, **IV**, **V**, **VI**, was also performed. The clamping levels, between 450 and 650 nm, and the linear transmission is given in figure 3.1.2, 3.1.3, and 3.1.4.

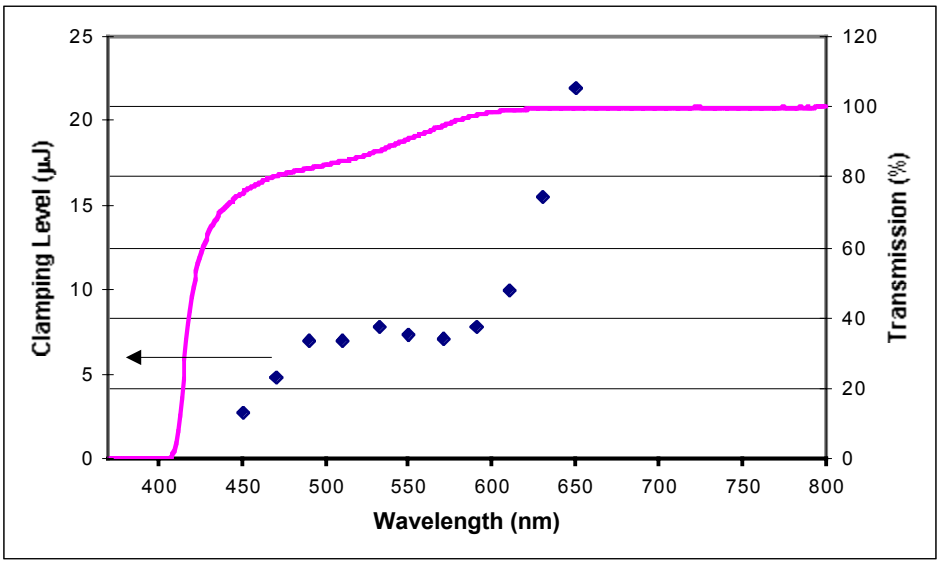

***Figure 3.1.2**. Clamping level and linear transmission for 2,5-Di(2-(4-pentylphenyl)ethynyl)-thiophene (**IV**)*

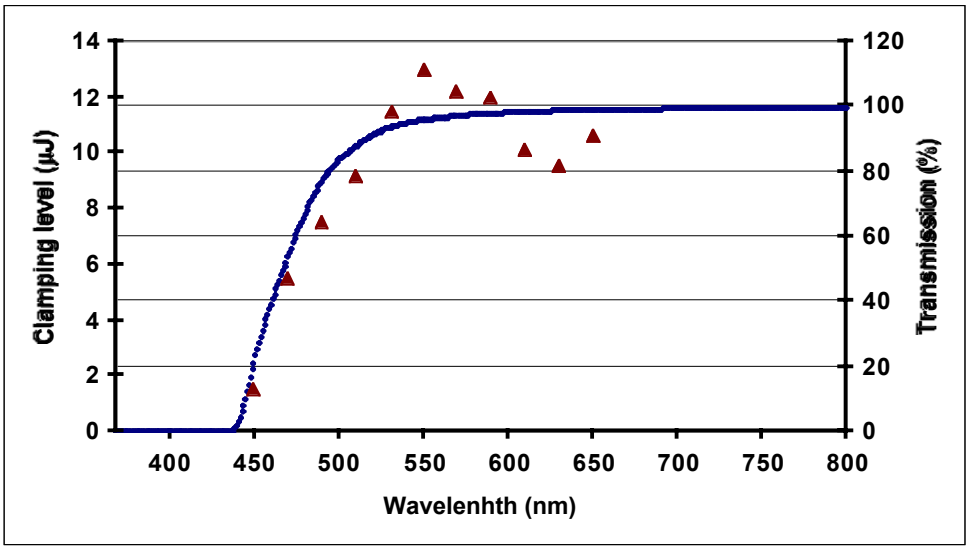

Figure 3.1.3. *Clamping level and linear transmission for 3-n-dodecyl-2,5-di(2-(4-(2-(4-pentylphenyl)ethynyl)phenyl)ethynyl)thiophene (**V**).*

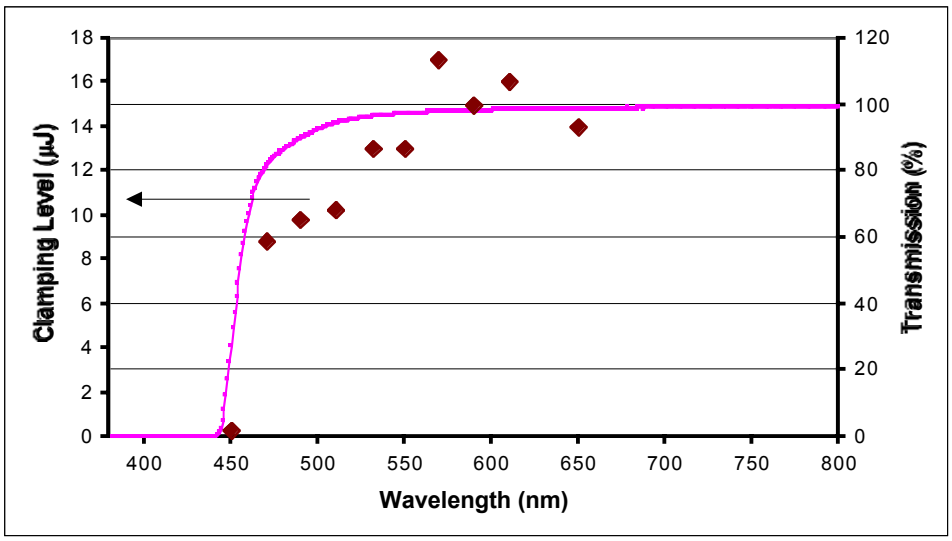

Figure 3.1.4*. Clamping level and linear transmission for 3-n-dodecyl-2,5-di(2-(4-(2-(4-(2-(4-pentylphenyl)ethynyl)phenyl)ethynyl)phenyl)ethynyl)thiophene (**VI**)*

A mixture (**MIX I**) of alkynylplatinum(II) was also investigated. The results are given in table 3.1.2. The input energy as a function of the transmitted energy at 532 nm is given in figure 3.1.5, and the linear transmission is given in figure 3.1.1.

Compound	% T @ 532 nm	% PT	Clamping
Mix 1	64	68	0.2 µJ @ 500 nm 0.5 µJ @ 532 nm 10 µJ @ 600 nm

Table 3.1.2. Experimental results on a mixture of alkynylplatinum(II) compounds

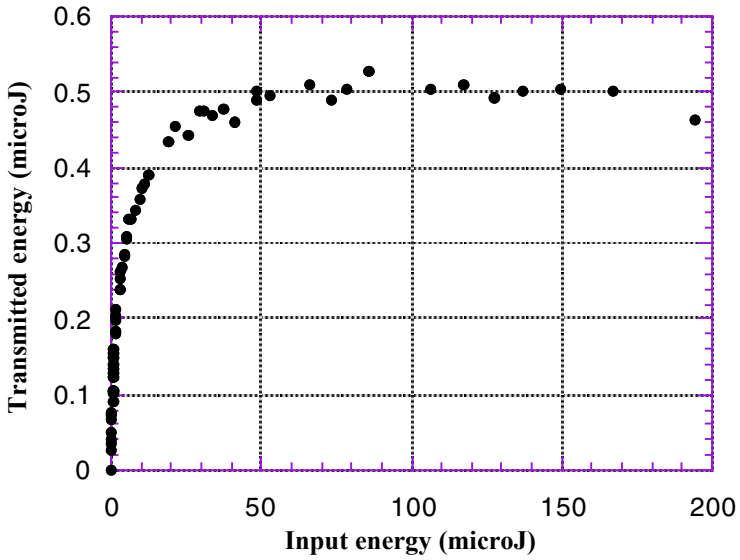

Figure 3.1.5.. Optical limiting response of a mixture of alkynylplatinum(II) compounds (**Mix 1**) @ 532 nm.

3.2. Theoretical modeling

The methodological development has progressed in parallel with applications of new compounds following the outline of the project plan. Several basic theoretical results have been achieved which we believe are of great value for applications later on in the project.

3.2.1 Methodological development

3.2.1.1. Role of coherent one-step versus incoherent two-step absorption for optical limiting

A dynamical density matrix based theory of two-photon absorption (TPA) of molecules and solutions has been worked out. The theory highlights the roles of pulse duration, dephasing and resonant conditions on the final TPA cross section, as well as of saturation - including a hierarchy of saturation intensities. The theory considers also the interplay between coherent one-step (two-photon absorption) and incoherent two-step (one-photon absorption to the first excited state followed by one-photon absorption from the first to the second excited state) contributions.

The numerical evaluation of the theory indicates that two-step off-resonant TPA going via one-photon off-resonant population of the first excited state can be of great importance for studies of condensed systems. The cross section of this process can exceed by a few orders of magnitude the one-step TPA for a long pulse. The physical reason of this can be found in the large dephasing broadening of resonances in solutions comparing to the inverse lifetime of the first excited state. The fast dephasing in solutions thus strongly suppresses the one-step resonant TPA and enhances the two-step TPA. The long lifetime of the first excited state thus makes the TPA very sensitive to the pulse duration. Indeed, in the case of short pulses the two-step TPA is strongly suppressed due to negligible population of the first excited state. This results in a suppression of the total TPA cross section for short pulses. Our analysis shows that long pulse measurements of the TPA cross section in the region of few hundred MW/cm^2 are not sufficient to carry out a correct extrapolation in the region of zero intensities. The reason for this lies in the strong saturation conditions in which such experiments are performed. The long pulse measurements of the TPA cross section thus have to be carried out for intensities smaller than the saturation intensities in order to ascertain a correct extrapolation to the zero intensity region. In that context we have shown that the shortening of the pulse duration shifts the saturation threshold to higher intensities. The analysis of some available experimental data leads to the conclusion that long pulse measurements often are made under a condition of strong saturation.
To summarize the findings in this project; we have predicted a breakdown of the conventional identification of TPA with one-step TPA for the long pulse regime

where two-step TPA can even dominate over the coherent one-step TPA process. The strong dependence of the two-step TPA on pulse duration leads to a quenching of this channel and to a suppression of the total TPA when the pulse duration time is shortened. The major role of the solvent is to enhance the off-resonant contributions to TPA caused by the collisional dephasing which occurs on a short time scale compared to the lifetime of the excited state. The findings have wide ramifications for optical limiting especially in the long-pulse regime.

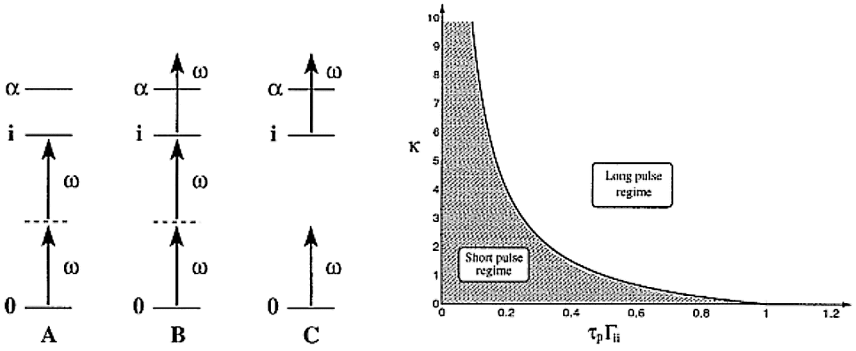

Figure 3.2.1.1. *Absorption channels and pulse duration dependence*

3.2.1.2. Generalized few-state models for two-photon absorption

Three-, and four-state models for two-photon absorption cross sections generalized to include dipolar direction information and polarization effects of the laser beams are presented. By introducing an effective dipole moment, which incorporates the directions of the transition dipole moments and the influence of additional strongly coupled excited states, we can distinguish between different effects leading to enhanced two-photon absorption. The generalization of the few-state models to include dipole moment directions and laser-beam polarization illustrates the need to consider the directions of the transition dipole moments. The numerical performance of these generalized few-state models for two-photon absorption have been evaluated at the density functional theory. and applied to *trans*-stilbene and donor-donor substituted *trans*-stilbene. We can through these few-state models gain new insight into the mechanisms behind the TPA, for example, we find that the increase of ground-to-excited state transition moment can be achieved by increasing the chain length, while the excited-to-excited state transition moment is more affected by the substituted donor groups. The alignment of these two transition moments is then an important factor.
We believe that these findings to be of great help in trying to screen candidate compounds with optical limiting capacity by simple means.

3.2.1.3. Development of propagator techniques for calculating the incoherent transition cross-sections

Consideration of the finite lifetime of the excited states has been made in developing the polarization propagator at both the electron uncorrelated and correlated levels of *ab initio* theory [9]. The values of the polarization propagator, also recognized as the linear polarizability, are complex with a real part relating to the refractive index of the sample and an imaginary part relating to the incoherent absorption of light quanta. The relevance of linear absorption in nonlinear optics is effectively expressed in terms of figures-of-merit. Such figures-of-merit have been calculated showing that the nonresonant linear absorption must be considered when the nonlinear optical quality of a material is to be assessed.

3.2.2. Applications

3.2.2.1. Use of effective core potentials for NLO properties

As an important step towards testing "real" coordination compounds for optical limiters we have explored the use of modern effective core-potentials (ECP) for NLO properties. We found that these provide excellent approximations to the all-electron values in all cases tested; errors for both polarizabilities and hyperpolarizabilities were typically of the order a few percent. The findings indicate considerable time savings in prediction of electric properties and of multi-photon absorption cross-sections of elements beyond the first row atoms. As an example of the new opportunities with ECP's we predicted size, order and dimensional relations for silicon cluster with computations of linear polarizabilities and second hyperpolarizabilities of 1-,2- and 3-dimensional hydrogen terminated clusters [10]. Successive enlargement of the clusters to embody an order of 50 silicon atoms plus bond saturating hydrogen atoms allows for extrapolation to bulk values of individual silicon atom contributions in the 1D- and 3D-cases.

3.2.2.2. Effects of relativity on linear and nonlinear polarizabilities

Relativistic calculations have been carried out for electric dipole moments, linear polarizabilities, and first- and second-order hyperpolarizabilities for the isovalent group VI (O--Po) dihydrides and group VII (F--At) monohydrides at three different levels: the time-dependent Dirac--Hartree--Fock approximation, the time-dependent Hartree--Fock approximation with a Douglas--Kroll transformed one-component Hamiltonian, and the time-dependent Hartree--Fock approximation with effective-core potentials. Results show that the scalar relativistic methods are qualitatively correct in their predictions of relativistic effects when compared to the fully relativistic 4-component approach. Within this project the justification of the ECP method with respect to inclusion of relativity is especially important, since, in

practice, its lower computational cost makes it the most realistic choice for the molecular systems of technical interest.

3.2.2.3. Effects of π-centers and symmetry on one-step two-photon absorption cross sections of organic chromophores

We have theoretically examined a series of organic molecules that exhibit large two-photon absorption cross sections in the visible region and that have been synthesized in different laboratories [11] (Figure 3.2.2.1)

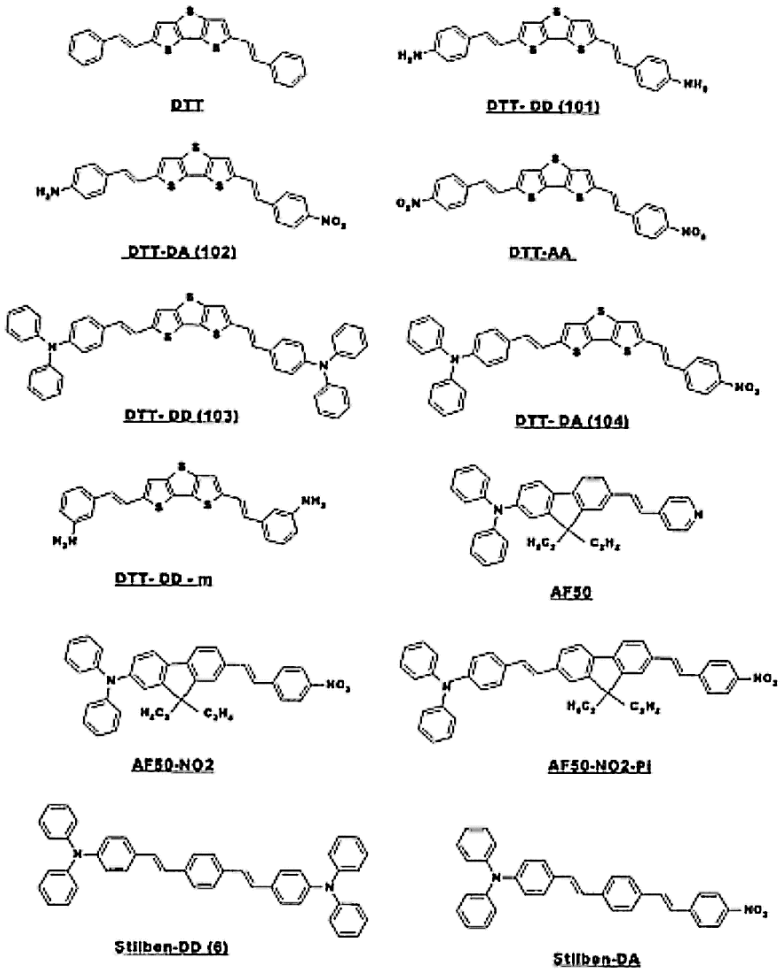

Figure 3.2.2.1. *Organic molecules with large TPA*

Our calculations have confirmed the experimental findings that π-centers play a most crucial role in the design of two-photon absorption materials. An electron-rich π-center attached to symmetrically substituted donors is found to constitute an optimal structure for maximizing the TPA cross sections in the visible region. For a given π-center, increasing the strength of symmetrically substituted donors will enhance the

TPA cross sections drastically. The TPA cross section can also be enhanced efficiently by increasing the dimensionality of the π-center, which in a way is equivalent to increase the strength of the π-center. The one-photon absorption spectra of all molecules studied were found to strongly correlate to the actual molecular length, while this was clearly not the case for two-photon absorption in the visible region. This implies that it is difficult to obtain quantitative information about TPA activity from the one-photon absorption spectra.
The chromophore based on dithienothiophene as π-center attached with symmetrical *N,N*-diphenylamine donors is found to have the largest two-photon cross section in the visible region among all known one-dimensional two-photon organic materials that have been reported in the literature.

3.2.2.4. One- and two-photon spectra of systematic donor/acceptor substituted alkynylplatinum(II) compounds

The development of the effective core potential (ECP) method has been a direct prerequisite for the calculations of linear and nonlinear absorption cross sections of alkynylplatinum(II) compounds: both platinum and phosphorous atoms are treated with ECP's. Results at the time-dependent Hartree--Fock (TDHF) and time-dependent density functional theory (TD-DFT) levels show a redshift of the linear absorption in the dimer as compared to the monomers. The absorption is directed along the conjugated ligands attached to the platinum atoms (Figure 3.2.2.2).

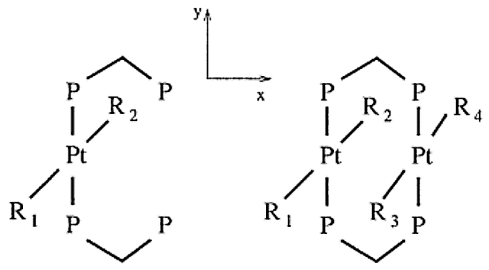

R_i	H
R_i	CH_3
R_i	C≡CH
R_i	C≡C—C_6H_5
R_i	C≡C—C_6H_4—NH_2
$R_1 = R_2$	C≡C—C_6H_4—NH_2
$R_3 = R_4$	C≡C—C_6H_4—NO_2
$R_1 = R_3$	C≡C—C_6H_4—NH_2
$R_2 = R_4$	C≡C—C_6H_4—NO_2

Figure 3.2.2.2. *Mononuclear and binuclear alkynylplatinum(II) compounds*

The nonlinear TPA is effective to the symmetric excited stated, and it is strongly enhanced by donor/acceptor substitutions (about one order of magnitude).

3.2.2.5. Density functional theory for non-linear optical processes in porphyrin based donor/acceptor systems

Among the several theoretical efforts taken, work on density functional theory (DFT) has formed an integral part. Although this theoretical methodology has found an enormous application area in contemporary chemistry (awarded Nobel prize 1998), little has been accomplished in the context of non-linear properties and nothing, to our knowledge, for the coherent many-photon process relevant for optical limiting and light control studied in this project. In an attempt to remedy this situation, and to further widen the application area of our toolbox, we have made a solid attempt to generalize our response theory for so-called ab initio reference states to a counterpart that is applicable for density functional theory, and we have succeeded with that. Our starting point was the so-called quasi-energy concept, which we have used to derive a time-dependent DFT for both linear and non-linear properties. The scope for applications is now considerably widened, for example to strongly correlated coordination compound systems and inorganic clusters. The incorporation of relativity through effective core potentials, see below, has also been accomplished.
Using the new tool, we have attacked porphyrin based donor-acceptor systems, which have been advocated as excellent candidates for optical limiting. Based on excellent results for the linear properties and one-photon spectra, we are now testing the applicability of non-linear properties and two-photon absorption (coherent one-step). Much of our current applications are focused to these type of systems. In a coming report we hope to provide a comprehensive account of results.

3.2.2.6. Photo-oxidation products of two-photon absorbers (AF50)

It is known that the organic compounds under continuous illumination loose their nonlinearity with time due to several different mechanisms. The understanding of such "failure" mechanisms for the OPL devices is thus evidently of importance for the design of device materials that are suitable for real applications, and something we have explored theoretically.
The photochemical reaction of large organic molecules is a very complicated issue. The identification of the final products is the first step towards a real understanding of the reaction mechanism. However, this can not be easily accomplished by experimental spectroscopic means alone, which is a general problem in the study of optical devices involving oxidation process. We have shown in a recent work that such a problem can be alleviated by combining theory and experiment. We have characterized the so-called AF50 molecule and its possible photo-oxidation products under UV exposure by computing IR and one-photon absorption spectra. Figure 3.2.2.3 shows two reaction schemes and their final products. We have found that for a pure AF50 molecule, the possible final oxidation products under the UV exposure at 325 nm are the ones that involve ring opening of the pyridine group. In comparison with the corresponding experimental IR and optical absorption spectra, a single

oxidation product, B3, is identified as the most possible oxidation product of AF50.

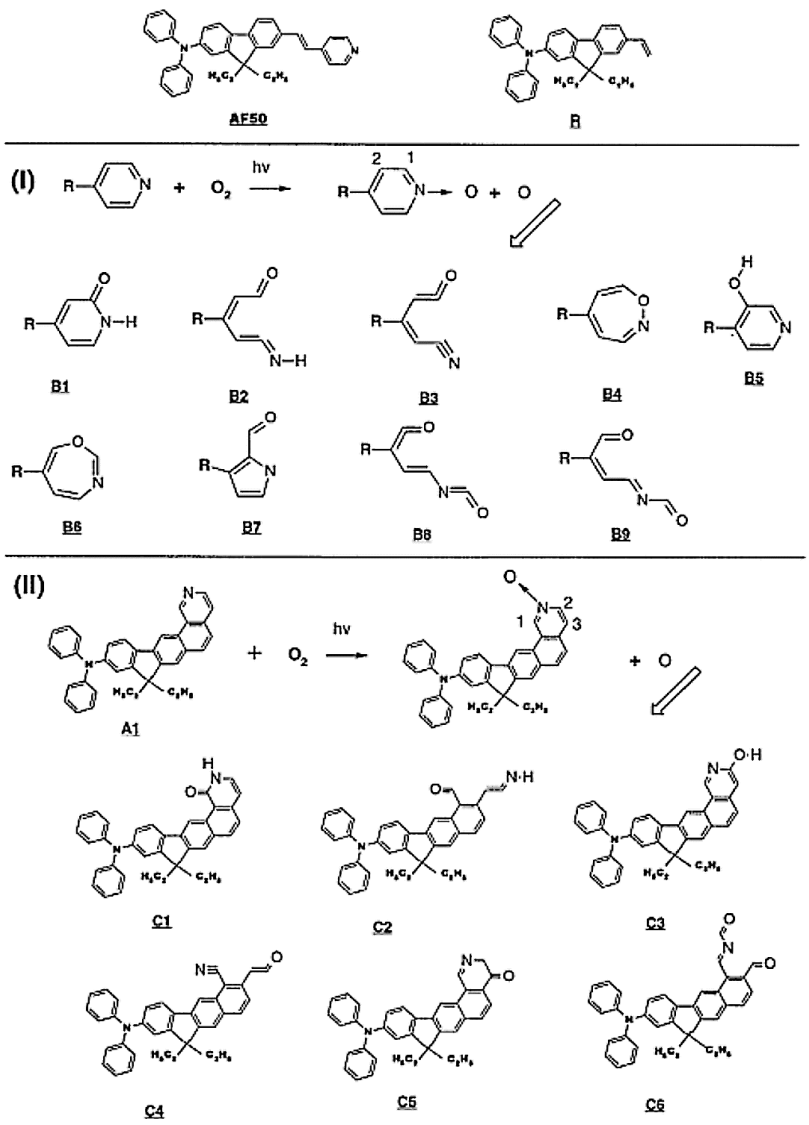

Figure 3.2.2.3. *Reaction schemes and molecular structures of possible oxidation products of AF 50*

3.2.2.7. Figures-of-merit for some charge transfer systems

Computationally tractable expressions for the evaluation of the linear response function in the multi-configurational self-consistent field approximation have been derived and implemented [9]. The finite lifetime of the electronically excited states has been considered and the linear response function is then convergent in the whole frequency region despite the presence of resonances or near-resonances. This is achieved by the incorporation of phenomenological damping factors that lead to complex response function values. The formulation does not depend on any particular assumptions about the perturbing fields, which may be time-independent or time-

dependent, internal or external, magnetic or electric, although the implementation is restricted to perturbations described by one-electron operators. Moreover, the approach taken is generally applicable to propagator methods that utilize other electronic structure methods. The indisputable advantage of the propagator technique is that there is no truncation of the number of excited states that are taken into account.

The present work includes applications in terms of the electric dipole polarizability of hydrogen fluoride, methane, *trans*-}butadiene, and three push-pull systems. The real part of the polarizability is connected with the refractive index and the imaginary part to the photon absorption (Figure 3.2.2.4)

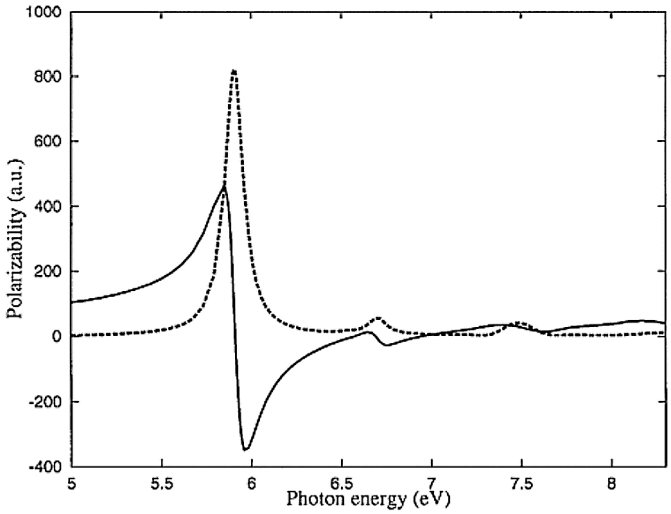

Figure 3.2.2.4. Real (solid line) and imaginary (dashed line) parts of the averaged polarizability of C_4H_6 at the RPA level with a lifetime broadening T = 1000 cm^{-1}

The present work is significant for the field of molecular design in nonlinear optics. In order for a material to be technically useful it needs not only to demonstrate large nonlinear responses but also small absorption. This consideration has been effectively described in terms of simple figures-of-merit, which relate nonlinear light scattering to linear and nonlinear light absorption. We argue that not only is the absorption at the operating frequency of a device to be considered but also the FOM at the resulting, scattered, frequency. When these factors are taken into account, the judged quality of a material may be changed in ways that would otherwise have been hard to predict. For instance the push-pull butadiene molecule, which shows both a greater nonlinear scattering response and a larger dispersion than *para*-nitroaniline, turns out to be the less effective of the two when absorption is taken into account, see Table 3.2.2.1. It is also shown that when the comparison of the two molecules is made one should take into account the nonlinear optical process where they are to be used. A further consideration to be made is that of nonlinear absorption; at this moment, we are not

able to address this issue since it involves the imaginary parts of the nonlinear polarizabilities, but we intend to undertake such calculations in the near future.

	C_4H_6	PNA	PPB	CUM
$\overline{\gamma}^R(0;0,0,0)$	14.81	26.97	30.07	53.20
E_g	0.2170	0.1844	0.1757	0.1024
dc-Kerr				
$\overline{\gamma}^R(-\omega;\omega,0,0)$	17.62	34.29	41.54	327.9
Dispersion	19%	27%	38%	516%
$\overline{\gamma}^R/\overline{\alpha}^I(-\omega;\omega)$	97.89	118.2	84.78	55.76
IDRI				
$\overline{\gamma}^R(-\omega;\omega,\omega,-\omega)$	21.40	48.06	67.23	–
Dispersion	44%	78%	124%	–
$\overline{\gamma}^R/\overline{\alpha}^I(-\omega;\omega)$	118.9	165.7	137.2	–
ESHG				
$\overline{\gamma}^R(-2\omega;\omega,\omega,0)$	26.94	69.62	113.1	–
Dispersion	82%	158%	276%	–
$\overline{\gamma}^R/\overline{\alpha}^I(-\omega;\omega)$	149.7	240.1	230.8	–
$\overline{\gamma}^R/\overline{\alpha}^I(-2\omega;2\omega)$	40.21	51.67	34.48	–
THG				
$\overline{\gamma}^R(-3\omega;\omega,\omega,\omega)$	92.06	–	–	–
Dispersion	522%	–	–	–
$\overline{\gamma}^R/\overline{\alpha}^I(-\omega;\omega)$	511.4	–	–	–
$\overline{\gamma}^R/\overline{\alpha}^I(-3\omega;3\omega)$	8.68	–	–	–

Table 3.2.2.1. Real part of the average second-order hyperpolarizability (the RPA value obtained in the infinite lifetime approximation) (10^8 a.u.) for some nonlinear optical processes at the dynamic frequency $\omega = 0.0656$ a.u., figure of merit (10^8 a.u.) relating nonlinear scattering to linear absorption (the linear absorption α^I is determined for $\Upsilon = 1000$ cm^{-1}), and gap energies (excitation energy for the dominating state in the linear absorption spectra).

4. Discussion

The lasers on the battlefield have the range and the power to cause damage to optical detectors. There is therefore a need of protective devices that can protect optical sensors without disturbing the information gathering.
In direct vision, *e.g.* through a sight, the human eye is the detector and can receive damaging laser doses. Protection of eyes requires broad band (400 - 700 nm) filters that can limit the laser beam to non-damaging energy levels. In this report we have investigated optical limiters based on nonlinear absorption. The limiting performance will depend on one or more mechanisms. Two-photon absorption (2PA), exited state absorption, self-defocusing, and, induced scattering are examples of optical limiting mechanisms. Useful materials should possess large nonlinear absorption and small linear absorption. However, the linear absorption is, though, needed to boost the nonlinear action. The position of the focus of the laser beam into the cell is of major importance. If the beam waist is set closer to the front cell window, lower clamping values is observed, but at the cost of a lower damage threshold to the front cell window. There is therefore much to be gained by protecting the cell windows from damage caused by decomposition products. If the focus can be set closer to the front cell window, thinner cells could be used, and this would result in higher linear transmission or that a higher concentration of the NLO compound could be used.

The assessment of the optical limiting performance of the compounds was investigated with the dyes in solution. Eleven new compounds were investigated. The clamping levels were recorded for wavelengths between 450 - 650 nm. A f/5 arrangement was used.

The thiophenes are organic compounds with extended π-delocalization (see section 2.3.2). They are usually yellow in color and have high photopic transmission. The thiophenes have shown results, which can match those obtained with organometallic compounds.
The best optical limiting result was obtained with a mixture of alkynylplatinum(II) compounds. This mixture showed low (< 1μJ) clamping values for a major part of the visible wavelengths. But, investigations at 600 nm showed a higher clamping value, ten times higher than our goal. The inability of a single material to function as a broad-band optical limiter can be solved by preparing mixtures of different compounds. And, if the chosen materials have complementary colors, the result can be a color neutral mixture.

5. Measurement uncertainties

Beam profile:
The beam profile is of major importance for the results of the measurements. In order to imitate a beam from a great distance, we strive to attain a circular top-hat profile.

Measurement precision:
In order to guarantee the stability and validity of the test-bed, control measurements were performed. The compound SINC (silicon-2,3-naphthalocyanine-bis(trihexyl-silyloxide), in toluene solution, 40% transmission, was used [6].
The alignment of the test-bed may result in small differences in the transmitted energy between realignments. This discrepancy is much smaller than the ones obtained due to the beam profile. The reproducibility of the results is assured through the relative measurements, although differences in the beam profile and alignment of the optics may result in small variations in the absolute energy values. We estimate a standard uncertainty of 25% of the energy values, mostly due to deviations from the top-hat beam profile of the laser beam. Scattering in the data of the investigated materials is assigned to impurities and is not considered.
Damage thresholds are probably quite sensitive to changes in the beam profile, but a thorough investigation is still needed.

6. References

1. Nonlinear Optics, 1999. **21**(1-4): p. 1-552.
2. McKay, T.J., et al., *cross sections for excited-state absorption in a Pt:ethynyl complex.* J. Opt. Soc. Am. B, 2001. **18**(3): p. 358.
3. Wang, P., et al., *Optical limiting properties of optically active phthalocyanine derivatives.* Chemical Physics Letters, 2001. **340**: p. 261-266.
4. Fougeanet, F. and D. Riehl, *Investigation of Optical Limiting Mechanisms in Carbon-black Suspensions.* Nonlinear Optics, 1999. **21**(1-4): p. 435-446.
5. Sliney, D.H., *Retinal injury from laser radiation.* Nonlinear Optics, 1999. **21**(1-4): p. 1-18.
6. Vincent, D., Nonlinear Optics, 1999. **21**: p. 413.
7. James, D.B., McEwan, K. J., Nonlinear Optics, 1999. **21**: p. 377.
8. Bartlett, N.R., Brown, J. L., Hsia, Y., Mueller, C. G., *Vision and Visual Perception*, ed. G.C. H. 1966: John Wiley and Sons; Inc.
9. Norman, P., Bishop, D. M., Jansen, H. J. A., Oddershede, J., J. Chem. Phys., 2001. **115**(15).
10. Jansik, B., Schimmelphenning, B., Norman, P., Mochizuki, Y., Luo, Y., Ågren, H., J. Phys. Chem., 2001.
11. Wang, C.K., Macak, P., Luo, Y., Ågren, H., J. Phys. Chem., 2001. **114**: p. 9813.

Appendix Synthesis

Alkynylplatinum(II) complexes

Overview:
$Pt(C{\equiv}C\text{-}p\text{-}C_6H_4C{\equiv}C\text{-}p\text{-}C_6H_4\text{-}n\text{-}C_5H_{11})_2(depm)$ was prepared by a reaction of $PtCl_2(depm)$ and $C_5H_{11}–p\text{-}C_6H_4–C{\equiv}C–p\text{-}C_6H_4–C{\equiv}C–H$ using *t*-BuOK in EtOH solution according to the scheme below.

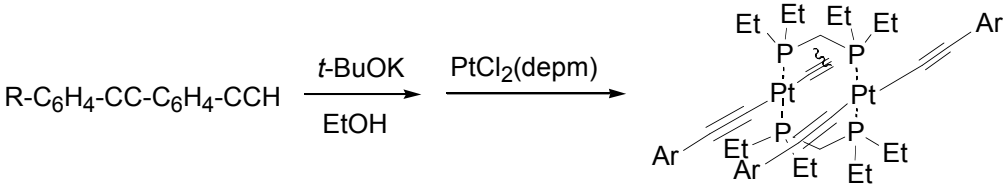

The ligand bis(diethylphosphino)methane, depm, $CH_2(PEt_2)_2$, was prepared according to a combination of earlier published methods in three steps:

$$Al + CH_2Cl_2 + CH_2I_2 \text{ (initiator)} \rightarrow Cl_2Al\text{-}CH_2\text{-}AlCl_2$$
$$Cl_2Al\text{-}CH_2\text{-}AlCl_2 + PCl_3 + POCl_3 \rightarrow Cl_2P\text{-}CH_2\text{-}PCl_2$$
$$Cl_2P\text{-}CH_2\text{-}PCl_2 + EtMgBr \rightarrow Et_2P\text{-}CH_2\text{-}PEt_2$$

$PtCl_2(depm)$ was synthesised from $PtCl_2[S(C_2H_5)_2]_2$ and depm in a ligand exchange reaction. The alkyne was prepared according to literature methods, as described in part elsewhere in this report.

$Pt(C{\equiv}C\text{-}p\text{-}C_6H_4C{\equiv}C\text{-}p\text{-}C_6H_4\text{-}n\text{-}C_5H_{11})_2(depm)$. Absolute ethanol (30 ml) was added to a mixture of $PtCl_2(depm)$ (0.14 g, 0.31 mmol), alkyne (0.17 g, 0.63 mmol) and *t*-BuOH (0.072 g, 0.64 mmol). The mixture was heated under reflux for 1 h and the resultant yellow solution was allowed to reach room temperature. The solution was stirred for ca. 10 h under argon during which time an orange precipitate formed. The precipitate was collected and purified by column chromatography on basic alumina using CH_2Cl_2/petroleum ether 1/2 as eluent. The yield of the orange solid product was 0.12 g (40 %).
^{1}H-NMR ($CDCl_3$): δ = 0.9 (t, 6H), 1.3 (m, 20H), 1.6 (p, 4H), 2.1 (m, 8H), 2.6 (t, 4H), 3.2 (t, 2H), 7.1 (d, 4H), 7.3 (s, 8H), 7.4 (d, 4H).

$Pt(C{\equiv}C\text{-}p\text{-}C_6H_4C{\equiv}C\text{-}p\text{-}C_6H_5)_2(depm)$ was prepared by the same procedure as described above, giving an orange solid in 25 % yield.
^{1}H-NMR ($CDCl_3$): δ = 1.3 (m, 12H), 2.1 (m, 8H), 3.2 (t, 2H), 7.3 (s, d, 12H), 7.5 (d, 4H).

Alkyne precursors for platinum(II) complexes

Overview scheme of the three-step preparation of 2-ethynyl-5-(4-pentylphenyl-ethynyl)thiophene:

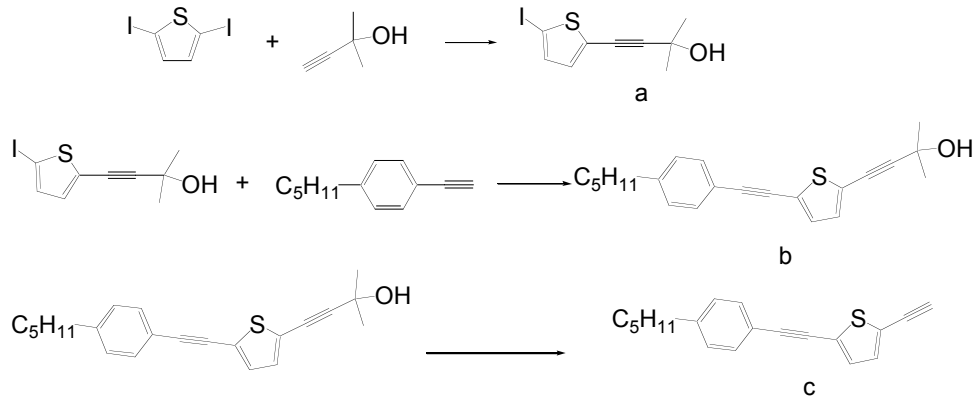

4-(5-Iodo-thiophen-2-yl)-2-methyl-3-butyn-2-ol (a). 2,5-diiodothiophene (5 g, 14.9 mmol) was dissolved in a mixture of 40 ml tetrahydrofuran and 20 ml triethylamine under argon. To the solution was added CuI (40 mg, 0.2 mmol), $Pd(PPh_3)_2Cl_2$ (95 mg, 0.13 mmol) and PPh_3 (0.1 g, 0.4 mmol). The alkyne (0.84 g, 10 mmol) was added dropwise and the reaction was allowed to run for 48 h at room temperature and at 60 °C for 24 h. The solution was cooled and poured into 100 ml 1M HCl. The organic layer was separated, washed with water, dried and the solvent evaporated. Chromatography on silica using a heptane/EtOAc 5/1 mixture as eluent (R_f= 0.3) gave the pure product (1.99 g, 68%) as an orange oil.
^{1}H-NMR ($CDCl_3$): δ = 1.57 (s, 6H), 2.09 (s, 1H), 6.8 (d, 1H), 7.07 (d, 1H).

2-Methyl-4-(5-(4-pentylphenylethynyl)thiophen-2-yl)-3-butyn-2-ol (b). The alcohol (1.0 g, 3.4 mmol) from the earlier step was added to a mixture of 15 ml tetrahydrofuran and 10 ml triethylamine under argon, followed by CuI (20 mg, 0.1 mmol), $Pd(PPh_3)_2Cl_2$ (50 mg, 0.07 mmol) and PPh_3 (0.04 g, 0.14 mmol). 4-Pentyl-1-ethynylbenzene (1.0 g, 5.8 mmol) was added dropwise to the solution which was then heated to reflux for 5 h. The solution was allowed to cool and poured into 50 ml 1M HCl. The organic layer was separated, washed with water, dried and the solvent evaporated. Chromatography of the organic residue on a silica column using heptane /EtOAc 5/1 as eluent (R_f = 0.4) yielded 0.98 g (86%) of pure product as a red oil.
^{1}H-NMR ($CDCl_3$): δ = 0.88 (t, 3H), 1.30 (m, 4H), 1.56 (m, 8H), 2.57 (t, 2H), 7.02 (d, 1H), 7.05 (d, 1H), 7.12 (d, 2H), 7.38 (d, 2H).

2-Ethynyl-5-(4-pentylphenylethynyl)thiophene (c). The alcohol (0.91 g, 2.7 mmol) was dissolved in 100 ml dry toluene under argon. NaH (0.22 g, 60% dispersion, 5.4 mmol) was added and 60 ml of the solvent was distilled off. The residue was carefully poured into 50 ml of cold 1M HCl. The organic phase was taken off, evaporated and filtered through a short silica column. Chromatography of the residue on a silica column using heptane as eluent gave pure product as white crystals, 220 mg (29%).
^{1}H-NMR ($CDCl_3$): δ = 0.94 (t, 3H), 1.35 (m, 4H), 1.65 (m, 2H), 2.63 (t, 2H), 3.38 (s, 1H), 7.11 (d, 1H), 7.05 (d, 1H), 7.17 (m, 3H), 7.45 (d, 2H).

Overview scheme of the four-step preparation of 4-(2-(5-methyl)-2-thiophenyl)ethynyl-1-ethynylbenzene:

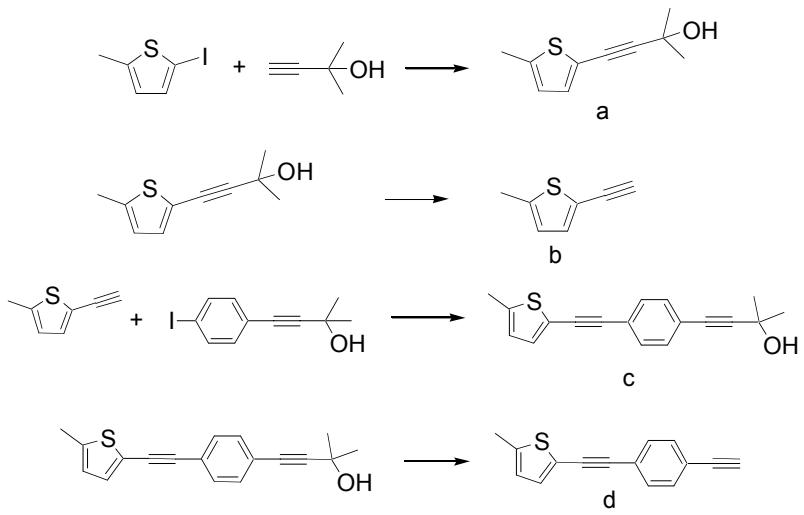

2-Methyl-4-(5-methylthiophen-2-yl)-3-butyn-2-ol (a). 2-Methyl-5-iodothiophene (3 g, 13.4 mmol) was dissolved in a mixture of tetrahydrofuran (10 ml) and triethylamine (10 ml) under argon. CuI (15 mg, 0.08 mmol), $Pd(PPh_3)_2Cl_2$ (40 mg, 0.06 mmol) and PPh_3 (40 mg, 0.15 mmol) was added, followed by dropwise addition of 2-methyl-3-butyn-2-ol. The reaction was stirred at room temperature overnight followed by reflux for 4 h. The solvent was removed and the residue dissolved in dichloromethane and washed with diluted HCl and water. Column chromatography of the crude product on silica using heptan/EtOAc 10/1 as eluent (R_f= 0.2) gave the product as a red oil. The yield was 2.3 g (95%).
^{1}H-NMR ($CDCl_3$): δ = 1.57 (s, 6H), 2.15 (s, 1H), 2.42 (s, 3H), 6.57 (d, 1H), 6.95 (d, 1H).

2-Ethynyl-5-methylthiophene (b). 2.5 g (14 mmol) of the alcohol from the preceding step was dissolved in 100 ml dry benzene. A 50 % NaH dispersion (1.3 g, 28 mmol) was added and the mixture slowly distilled until half of the volume remained. The solution was cautiously poured into 50 ml cold 1 M HCl and extracted with dichloromethane. The organic layer was separated, washed with water, dried and the solvent evaporated. Purification on a silica column using heptane as eluent gave 1.2 g (70%) of product.
^{1}H-NMR ($CDCl_3$): δ = 2.45 (s, 3H), 3.28 (s, 1H), 6.14 (d, 1H), 7.08 (d, 1H).

2-Methyl-4-(4-(5-methylthiophen-2-yl-ethynyl)-phenyl)- 3-butyn-2-ol (c). 4-(4-iodophenyl)-2-methyl-3-butyn-2-ol (3.5 g, 12.3 mmol) was dissolved in a mixture of 20 ml dry tetrahydrofuran and 10 ml dry triethylamine under argon. To this solution was added CuI (20 mg, 0.1 mmol), $Pd(PPh_3)_2Cl_2$ (50 mg, 0.07 mmol) and PPh_3 (40 mg, 0.15 mmol). Subsequently, 2-ethynyl-5-methylthiophene (1g, 8.2 mmol) was added droppwise. The solution was stirred overnight at room temperature,

refluxed for 4 h, cooled and poured into 50 ml 1M HCl. The organic phase was removed, washed with water, dried and the solvent was evaporated. Chromatography on a silica column using heptane/EtOAc 10/1 yielded 0.82 g (36%) pale yellow crystals.
^{1}H-NMR ($CDCl_3$): δ = 1.60 (s, 6H), 2.45 (s, 3H), 2.51 (s, 1H), 6.29 (d, 1H), 7.07 (d, 1H), 7.33-7.40 (dd, 4H).

4-(2-(5-Methyl)thiophen-2-yl)ethynyl-1-ethynylbenzene (d). The alcohol (0.69 g, 2.46 mmol) from the preceding reaction was dissolved in 100 ml dry benzene. A 50 % NaH dispersion (0.12 g, 5 mmol) was added and solvent distilled until half of the volume remained. The residue was cautiously poured into 50 ml cold 1M HCl and extracted with dichloromethane. After drying and evaporation, the brown crude product was filtered through a short silica column using hexane. This afforded a colorless filtrate, which was further purified on silica using hexane (R_f = 0.35). The yield was 0.38 g (70%).
^{1}H-NMR ($CDCl_3$): δ = 2.47 (s, 3H), 3.14 (s, 1H), 6.64 (d, 1H), 7.07 (d, 1H), 7.42 (m 4H).

Di- and trialkynylthiophenes

The alkynes were prepared according to standard procedures and were coupled to 2,5-dibromo-3-dodecylthiophene or 2,3,5-tribromothiophene using Pd and Cu(I) catalysts (Sonogashira coupling reaction).

2-Methyl-4-(4-(4-pentylphenylethynyl)phenyl)-3-butyn-2-ol. 4-(4-Iodophenyl)-2-methyl-3-butyn-2-ol (4.1 g, 14 mmol) was added to a mixture of 80 ml pyridine and 80 ml triethylamine. To the solution was added $PdCl_2(PPh_3)_2$ (20 mg, 0.29 mmol), PPh_3 (60 mg, 0.11 mmol) and CuI (55 mg, 0.29 mmol). 4-Pentylphenylacetylene (4.8 g, 28 mmol) was added dropwise to the mixture and the reaction was stirred for 20 h at room temperature. The solvent was removed under reduced pressure and the resultant pale brown solid was collected using ether, washed twice with 50 ml dilute HCl and twice with 50 ml water. After drying, recrystallisation of the brownish solid gave 4.1 g (89%) of white fluffy product. R_f = 0.25 (heptan/EtOAc 10/1).
^{1}H NMR ($CDCl_3$): δ = 0.87 (t, 3H), 1.29 (m, 4H), 1.60 (m, 8H), 2.59 (t, 3H), 7.15 (d, 2H), 7.37 (d, 2H), 7.42 (t, 4H).

1-Ethynyl-4-(4-pentylphenylethynyl)benzene. The protected alkyne (1.39 g, 4.2 mmol) was dissolved in 100 ml benzene. NaH (0.5 g, 50% dispersion in oil) was added and the mixture was slowly distilled until 50 ml of the distillate had been collected. The solution was allowed to cool and was then poured into cold water. The organic phase was removed, dried and evaporated. The brown-yellow product was passed through a silica column (hexane/ EtOAc 10/1). The resultant yellow product was passed through a short alumina column using hexane as eluent. This gave 1.0 g

(88%) of white product. R_f = 0.9 (heptan/EtOAc 10:1). IR: 3270, 2923, 2213, 1598, 1514, 1464 cm^{-1}.
^1H NMR ($CDCl_3$): δ = 0.87 (t, 3H), 1.30 (m, 4H), 1.59 (m, 2H), 3.15 (s, 1H), 7.16 (d, 2H), 7.40-7.44 (m, 4H).

The alkyne 1-Ethynyl-4-(4-(4-pentylphenylethynyl)phenylethynyl)benzene was prepared by the same procedure as described above. ^1H NMR and IR data for the alcohol and the alkyne is given below.

2-Methyl-4-(4-(4-(4-pentylphenylethynyl)phenylethynyl)phenyl)-3-butyn-2-ol.
^1H NMR ($CDCl_3$): δ = 0.83 (t, 3H), 1.26 (m, 4H), 1.56 (m, 8H), 1.94 (s, 1H), 2.55 (t, 2H), 7.09 (d, 2H), 7.31-7.42 (m, 10H).
1-Ethynyl-4-(4-(4-pentylphenylethynyl)phenylethynyl)benzene.
IR: 3268, 2915, 1926, 1517, 1407, 1267 cm^{-1}.
^1H NMR (CDCl3): δ = 0.87 (t, 3H), 1.30 (m, 4H), 1.60 (m, 2H), 2.59 (t, 2H), 3.16 (s, 1H), 7.16 (d, 2H), 7.41-7.48 (m, 10H).

2,5-Di-(4-pentylphenylethynyl)thiophene. 2,5-Diiodothiophene (1.5 g, 4.5 mmol) was dissolved in a mixture of 20 ml pyridine and 20 ml triethylamine under argon. $PdCl_2(PPh_3)_2$ (60 mg, 0.085 mmol), PPh_3 (70 mg, 0.27 mmol) and CuI (25 mg, 0.13 mmol) was added, followed by dropwise addition of 1-ethynyl-4-pentylbenzene (2 g, 12 mmol). The reaction was stirred for 48 h at room temperature. The solvent was removed and the residue dissolved in CH_2Cl_2 and washed with diluted HCl and water. The organic phase was dried and evaporated, and the product was purified on a silica column using heptane as eluent. This gave 0.78 g (41%) of a pinkish product, mp 62-64ºC. IR: 2919, 2194, 1747, 1649, 1479, 1203 cm^{-1}.
^1H NMR ($CDCl_3$): δ = 0.88 (t, 6H), 1.32 (m, 8H), 1.62 (m, 4H), 2.61 (t, 4H), 7.12 (s, 1H), 7.15 (d, 4H), 7.42 (d, 4H).

3-Dodecyl-2,5-di-(4-(4-pentylphenylethynyl)-phenylethynyl)-thiophene.
To a solution of 3-*n*-dodecyl-2,5-dibromothiophene (0.38 g, 0.9 mmol) in 10 ml pyridine and 10 ml triethylamine under argon was added $PdCl_2(PPh_3)_2$ (50 mg, 0.074 mmol), PPh_3 (40 mg, 0.15 mmol) and CuI (20 mg, 0.11 mmol). The alkyne was dissolved in 20 ml pyridine and added dropwise over a period of 2 h. The solution was stirred 48 h at room temperature and 2 h at 50 °C. The solvent was removed and the residue dissolved in CH_2Cl_2 and washed with diluted HCl and water. The organic phase was dried and the solvent evaporated. The solid was dissolved in a hot solution of 5 % EtOAc in hexane and filtered through a short silica column (R_f = 0.25 in hexane). Repeated recrystalization from hot hexane yielded 0.33 g (46 %) of yellow product.
^1H NMR ($CDCl_3$): δ = 0.88 (m, 9H), 1.25-1.33 (m, 26H), 1.61 (m, 6H), 2.61 (t, 4H), 2.72 (t, 2H), 7.06, (s, 1H), 7.15 (d, 4H), 7.43-7.50 (m, 12H).

3-Dodecyl-2,5-di-(4-(4-(4-pentylphenylethynyl)-phenylethynyl)-phenylethynyl)-thiophene. To a solution of 3-*n*-dodecyl-2,5-dibromothiophene (0.11 g, 0.27 mmol) in 5 ml toluene and 5 ml triethylamine under argon was added $PdCl_2(PPh_3)_2$ (15 mg, 0.022 mmol), PPh_3 (14 mg, 0.054 mmol) and CuI (6 mg, 0.032 mmol). The alkyne was dissolved in warm toluene and added dropwise over a period of 2 h. After being heated to 90 °C for 48 h, the solvent was removed and the residue dissolved in CH_2Cl_2 and washed as described above, followed by drying and evaporation of the solvent. The solid was dissolved in hot 50 % toluene in heptane and filtered through a short silica column using heptane/EtOAc 50/50 as eluent (R_f = 0.4, heptane/EtOAc 10/1). The volume of the filtrate was reduced and a yellow precipitate was collected. The solid was recrystallized by dissolving it in hot CH_2Cl_2 and adding hexane until a precipitate was formed. The yield of the yellow product was 75 mg (28 %).
^{1}H NMR ($CDCl_3$): δ = 0.88 (m, 9H), 1.25-1.33 (m, 26H), 1.63 (m, 6H), 2.62 (t, 4H), 2.73 (t, 2H), 7.08 (s, 1H), 7.15 (d, 4H), 7.43-7.50 (m, 20H).

Two dinitrothiophenes have been prepared by one-step reactions starting from commercially available reagents.
2,5-Di(4-pentylphenylethynyl)-3,4-dinitrothiophene was obtained as shown in the scheme below.

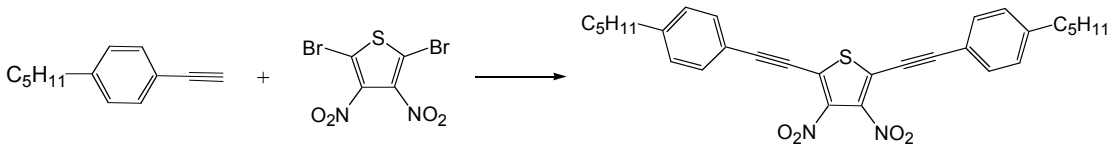

2,5-Di(4-pentylphenylethynyl)-3,4-dinitrothiophene. 2,5-Dibromo-3,4-dinitrothiophene (0.5 g, 1.5 mmol) was dissolved in a mixture of 10 ml tetrahydrofuran and 10 ml triethylamine under argon atmosphere.
To the solution was added CuI (20 mg, 0.1 mmol), $Pd(PPh_3)_2Cl_2$ (40 mg, 0.06 mmol) and PPh_3 (30 mg, 0.12 mmol), followed by dropwise addition of the alkyne (0.8 g, 4.5 mmol). The color of the solution changed rapidly from pale yellow to red. The reaction mixture was stirred for 20 h at room temperature and was refluxed for an additional 4 h. The solution was cooled and poured into 50 ml 1M HCl. The organic layer was dried an evaporated. Column chromatography of the dark crude product on silica, followed by recrystalization from hexane afforded the desired product as orange crystals. The yield was 100 mg (0.19 mmol).
^{1}H-NMR ($CDCl_3$): δ = 0.89 (t, 6H), 1.31 (m, 8H), 1.61 (m, 4H), 2.61 (t, 4H), 7.20 (d, 4H), 7.47 (d, 4H).
^{13}C-NMR ($CDCl_3$): δ = 14.7, 23.2, 31.5, 32.1, 36.8, 77.4, 106.6, 118.2, 123.3, 129.6, 133.0, 141.0, 147.2.
IR: 2925, 2854, 2202, 1548, 1402, 1327 cm^{-1}.

2,5-Di(4-aminophenylethynyl)-3,4-dinitrothiophene was obtained as shown in the scheme below.

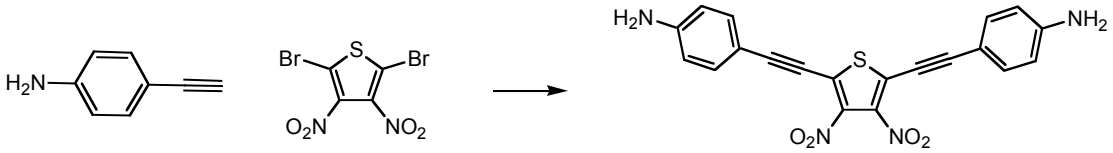

2,5-Di(4-aminophenylethynyl)-3,4-dinitrothiophene. 2.5-Dibromo-3.4-dinitrothiophene 0.5 g (1.5 mmol) was dissolved in a mixture of 10 ml tetrahydrofuran and 10 ml triethylamine under argon atmosphere. To the solution was added CuI (20 mg, 0.1 mmol), $Pd(PPh_3)_2Cl_2$ (40 mg, 0.06 mmol) and PPh_3 (30 mg, 0.12 mmol). The alkyne (0.53 g, 4.5 mmol) was dissolved in 5 ml THF and added dropwise. The solution rapidly changed color from pale yellow to dark red. The reaction mixture was stirred at room temperature for 48 h and subsequently poured into 50 ml 1M HCl. The organic layer was dried and evaporated. Column chromatography of the dark crude product on silica, followed by repeated recrystalization from dichloromethane and methanol afforded the desired product as a dark powder.
^{1}H-NMR (THF-d_8): δ = 5.34 (s, 4H), 6.57 (d, 4H), 7.27 (d, 4H).
^{13}C-NMR (THF-d_8): δ = 74.9, 105.4, 107.0, 112.4, 121.2, 132.1, 132.6, 150.4.
IR: 3473, 3375, 2166, 1595, 1535, 1392, 1307, 1172, 1132 cm^{-1}.

2,3,5-tri(1-(4-pentylphenyl)ethynyl)thiophene was obtained in two steps by the same procedure as described above for the disubstituted thiophenes.

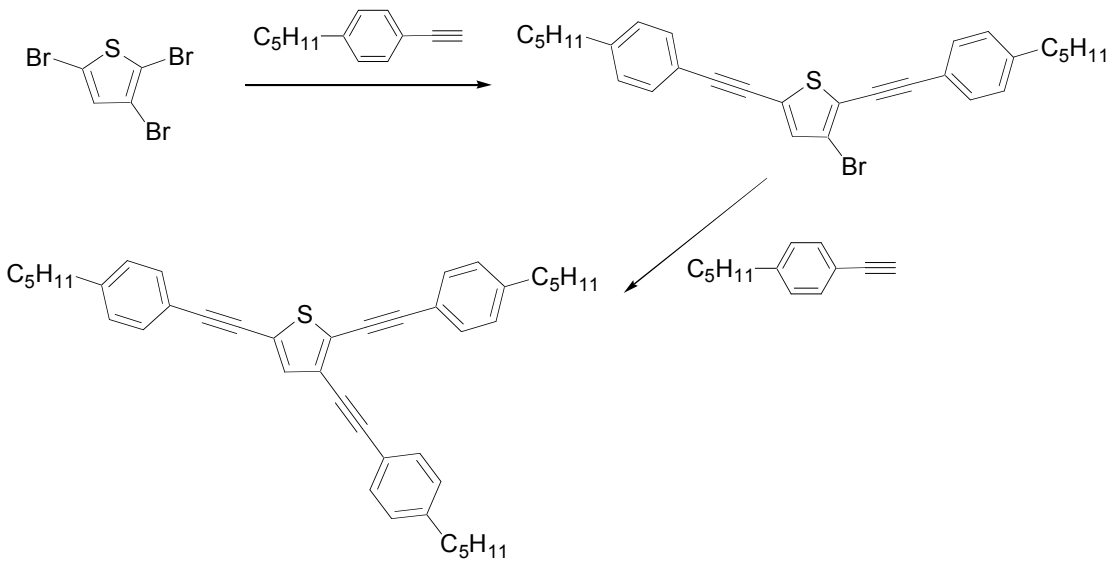

3-bromo-2,5-di(4-pentylphenylethynyl)thiophene. The tribromothiophene (0.62 g, 1.9 mmol) was dissolved in 15 ml pyridine and 10 ml triethylamine together with CuI (11 mg, 0.06 mmol), $PdCl_2(PPh_3)_2$ (32 mg, 0.045 mmol) and PPh_3 (24 mg, 0.09 mmol) under argon atmosphere. 4-Pentyl-1-ethynylbenzene (1.5 g, 8.7 mmol) was added dropwise. After 64 h at room temperature, the solvent was removed and the residue dissolved in CH_2Cl_2. The organic phase was washed with 1M HCl and water, dried and evaporated. The crude product was dissolved in heptane and filtered through a short silica column followed by chromatography on a silica column using heptane. The yield of the disubstituted thiophene was 380 mg.
^{1}H NMR ($CDCl_3$): δ = 0.87 (t, 6H), 1.30 (m, 8H), 1.59 (m, 4H), 2.61 (t, 4H), 7.1 (s, 1H), 7.15 (dd, 4H), 7.42 (d, 2H), 7.46 (d, 2H).

2,3,5-tri(4-pentylphenylethynyl)thiophene. The disubstituted thiophene (100 mg, 0.2 mmol) was dissolved in a mixture of pyridine (10 ml) and triethylamine (10 ml) under argon. CuI (3 mg, 0.012 mmol), $PdCl_2(PPh_3)_2$ (5 mg, 0.008 mmol) and PPh_3 (4 mg, 0.015 mmol) was added. 4-Pentyl-1-ethynylbenzene (70 mg) was added dropwise. The reaction was stirred for 5 days at 70 °C. The solvent was removed and the residue dissolved in CH_2Cl_2.The solution was washed with 50 ml 1M HCl and water, and the organic phase was dried and evaporated. Chromatography of the residue on a silica column, using heptane as eluent, gave a yellow oil (R_f = 0.15). The yield was 40 mg (34%).
^{1}H NMR ($CDCl_3$): δ = 0.89 (t, 9H), 1.31 (m, 12H), 1.61 (m, 6H), 2.61 (t, 6H), 7.15 (d, 6H), 7.19 (s, 1H), 7.42 (d, 2H), 7.41-7.47 (m, 6H).